BMC Genomics

RESEARCH Open Access

Dissecting the population structure, diversity and genetic architecture of rust resistance in wild emmer wheat (*Triticum turgidum* subsp. *dicoccoides*)

Laxman Adhikari[1,2], Pablo D. Olivera[3], John Raupp[2], Hanan Sela[4], Assaf Distelfeld[4], Marco Maccaferri[5], Matteo Bozzoli[5], Elisabetta Mazzucotelli[6], Andrea Brandolini[7], Roberto Tuberosa[5], Hakan Özkan[8,9], Brande B. H. Wulff[1*], Brian J. Steffenson[3*] and Jesse Poland[1,2*]

Abstract

Background Wild emmer wheat (*Triticum turgidum* subsp. *dicoccoides*, WEW) was one of the first crops domesticated in the Neolithic revolution that shifted humanity to agrarian societies. Understanding its population genomics has both evolutionary significance and direct relevance to wheat improvement. Leveraging whole-genome sequencing (WGS) data from 291 accessions (~ 9.5x coverage), we identified 3.4 million high-quality SNPs for population genomics, evolutionary analysis, and genome-wide association studies (GWAS) of seedling-stage resistance to five races each of the stem, leaf, and stripe rust pathogens.

Results Phylogenetic, principal component, and population structure analyses revealed three distinct WEW subgroups: the Northern Population (NP), Southern Levant (SL), and a highly differentiated *judaicum* subgroup consisting of accessions near the Sea of Galilee. Diversity and pairwise F_{ST} analyses highlighted varying divergence among these subpopulations. The SL accessions exhibited higher resistance to all races of the three rust pathogens compared to the *judaicum* and NP. The SL accessions also exhibited the highest frequency of resistance to all rust pathogens, whereas NP lacked stem rust resistance but retained resistance to some leaf and stripe rust races. GWAS identified 27, 26, and 41 significant loci associated with stem, leaf, and stripe rust resistance, respectively, most of which were novel. A major resistance hotspot was identified on chromosome 1BS (~ 50–100 Mb), associated with multiple races of different rust pathogens, suggesting the presence of shared or tightly linked resistance factors in the region. The most significant loci explained up to 73% of the phenotypic variation, with some conferring race-specific and others multi-race resistance. Notably, several accessions exhibited broad-spectrum resistance, including lines

*Correspondence:
Brande B. H. Wulff
brande.wulff@kaust.edu.sa
Brian J. Steffenson
bsteffen@umn.edu
Jesse Poland
jesse.poland@kaust.edu.sa

Full list of author information is available at the end of the article

resistant to all stripe rust races, others resistant to multiple leaf and stem rust races, and a subset combining resistance to multiple rust species, representing valuable germplasm for breeding durable resistance.

Conclusions This study provides a comprehensive genomic and phenotypic characterization of WEW, uncovering its population structure and identifying valuable genetic resources for rust resistance. The identified loci and resistant accessions offer key opportunities for the targeted introgression of novel resistance genes into cultivated wheat, contributing to durable and sustainable global wheat production.

Keywords Wild Emmer Wheat, *Triticum turgidum* subsp. *dicoccoides*, Whole-genome sequencing, Population structure, GWAS, Stem rust, Leaf rust, Stripe rust, Wild emmer subgroup *judaicum*

Background

Adverse climate, limited arable land, water scarcity, soil degradation, and biotic and abiotic stresses pose major challenges to sustainable crop production. Stem rust (*Puccinia graminis* Pers.:Pers. f. sp. *tritici* Eriks. & E. Henn.), leaf rust (*P. triticina* Eriks.), and stripe rust (*P. striiformis* Westend. f. sp. *tritici* Eriks.) cause significant global losses in bread wheat (*Triticum aestivum* L.) and durum wheat (*T. turgidum* subsp. *durum*). For instance, more than 90% of varieties were found susceptible to the stem rust isolate Ug99 following its discovery in Africa [1]. Similarly, a recent probabilistic bio-economic assessment suggests that over 90% of global wheat production is vulnerable to leaf rust [2], and stripe rust threatens 88% of worldwide wheat varieties due to increased spread of virulent races over the past six decades [3]. Despite the efforts to breed wheat cultivars resistant to these devastating diseases, the genetic diversity for disease resistance in wheat remains insufficient for the long-term control of these variable rust pathogens. This limitation primarily stems from constraints imposed by the domestication bottleneck and intense selection practices used in breeding. In contrast, wild wheat progenitors and relatives harbor rich genetic variation, offering valuable resources to overcome the constraints in cultivated wheat [4–6].

Wild emmer wheat (*T. turgidum* subsp. *dicoccoides*), henceforth referred to as WEW, is among the earliest domesticated crops [7]. Its natural distribution spans the western Fertile Crescent, including Lebanon, Syria, the Southern Levant, southeastern Anatolia, and mountainous regions of eastern Iraq and western Iran [8]. Tetraploid WEW (2n = 4x = 28) is the progenitor of cultivated tetraploid wheat and contributed the A and B genomes to hexaploid bread wheat (AABBDD), while *Aegilops tauschii* contributed the D genome [9, 10]. WEW exhibits extensive phenotypic variation for key agronomic traits, particularly disease resistance. For example, two genes (*Pm41* and *Pm36*) have been identified for powdery mildew resistance [9, 11], two (*Yr15* and *Yr84*) for seedling-stage stripe rust resistance [12, 13], and two (*Yr36*, *Yr-SM139*) for adult-stage stripe rust resistance [14, 15]. A population derived from a cross between WEW and susceptible durum wheat also showed resistance to leaf and stem rust [16]. Thus, evaluating WEW germplasm offers great potential for harnessing novel variation for disease resistance.

Understanding the population structure of wild emmer wheat (WEW) using a robust whole-genome sequencing (WGS) dataset is essential for effectively exploiting genetic resources in bread and durum wheat breeding. Clarifying the relationship between wild and domesticated emmer in larger populations also aids the selection of target germplasm. Previous studies, relying on morphology or limited genetic markers, have been insufficient to reach definitive conclusions; for example, the domestication site of emmer remains debated as southeastern Anatolia, the southern Levant (SL), or other regions have been posited as sites of domestication [7]. Disease-related associations and quantitative trait loci (QTL) analyses in WEW have also been limited by small sample sizes and low-coverage methods such as genotyping-by-sequencing (GBS) [17]. Conducting a Genome-wide association study (GWAS) on a larger, diverse panel with single nucleotide polymorphisms (SNPs) is therefore invaluable for identifying novel loci.

Hence, the primary objectives of this study were to: (i) assemble and whole-genome sequence a representative WEW panel capturing broad geographical distribution and diversity; (ii) analyze population structure and diversity within the WGS panel; (iii) perform a comprehensive GWAS to identify genomic regions conferring resistance to five races of each of the three rust pathogens; and (iv) provide extensive sequencing and phenotypic data to the research community.

Methods

Plant materials and pathogen isolates

We developed a genetically diverse panel of WEW comprising 291 accessions from four gene banks: 137 from the Wheat Genetics Resource Center (WGRC) at Kansas State University (KSU) in Manhattan KS, USA; 76 from the USDA-ARS National Small Grains Collection (NSGC) in Aberdeen, ID, USA; 58 from the Council for Agricultural Research and Agricultural Economics Analysis (CREA) in Fiorenzuola d'Arda, Italy, originally obtained from the National BioResource Project (NBRP)

in Komugi, Kyoto, Japan; and 20 additional accessions directly from NBRP. Accessions were selected to cover the species' geographic range including southeastern Anatolia, Iraq, Iran, and the southern Levant (Fig. 1a-b), and were advanced through single-seed descent in the greenhouse to ensure high homozygosity. A representative spike of WEW is shown in Fig. 1c. Passport data and disease scores are given in Supplementary Table S1.

The NSGC accessions were chosen based on prior stem rust resistance evaluations and were also selected from diverse regions. The panel was evaluated at the seedling stage against five races each of *P. g.* f. sp. *tritici*, *P. triticina*, and *P. s.* f. sp. *tritici* (Fig. 1d-f; Supplementary Note S1 and Supplementary Table S2).

In a separate analysis, we used genotyping-by-sequencing (GBS) data from 483 WGRC accessions

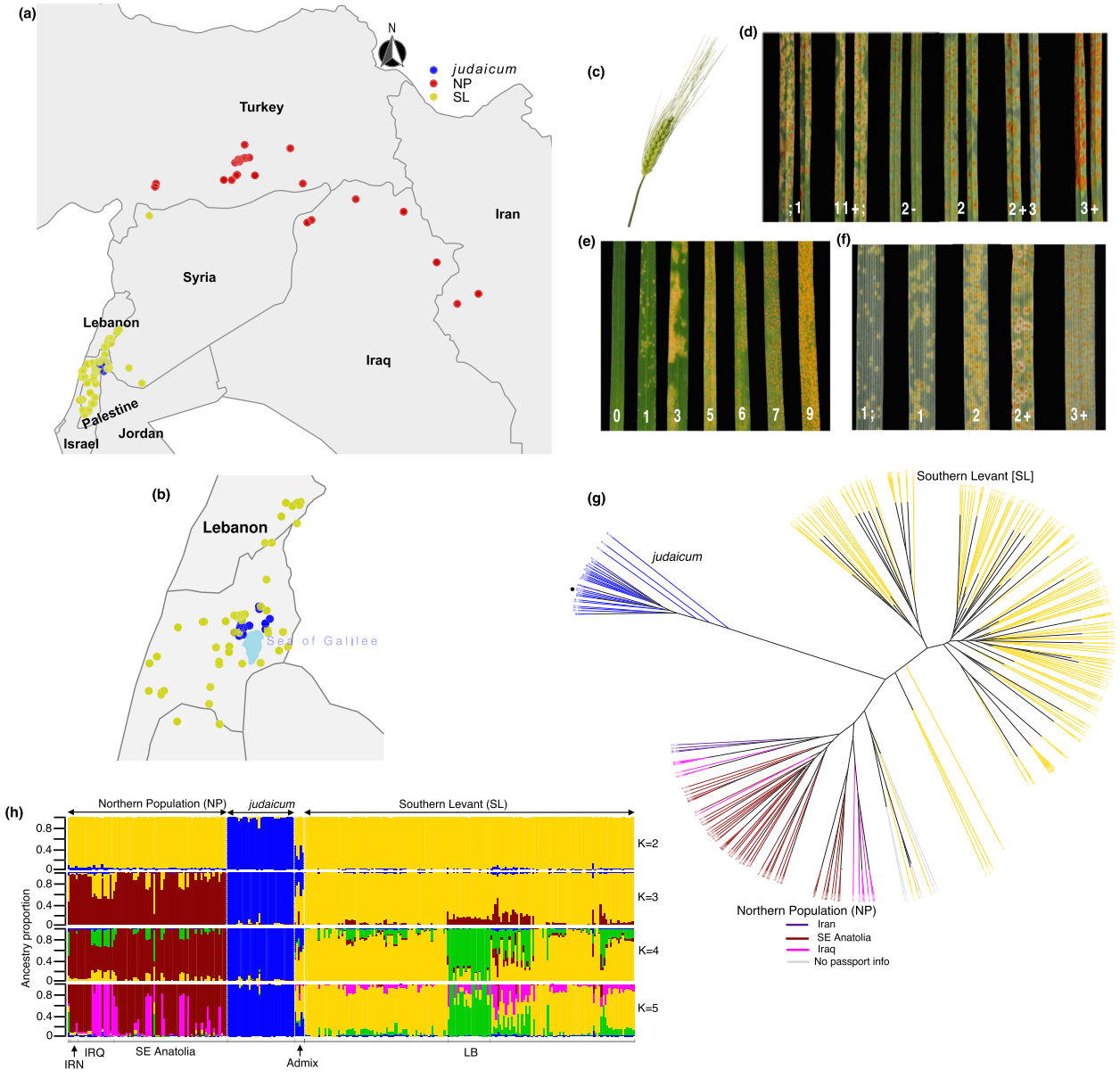

Fig. 1 Geographic distribution, disease scoring, and population structure of Wild Emmer Wheat (WEW). **a** Geographic distribution of WEW accessions included in the panel. **b** Enlarged view of the region around the Sea of Galilee (Lake Tiberias), highlighting the southern Levant and *judaicum* subgroups. **c** Spike morphology of a representative WEW accession in the panel. **d** Examples of stem rust infection types in WEW. **e** Examples of stripe rust infection types in WEW. **f** Examples of leaf rust infection types in WEW. **g** Phylogenetic tree with branches colored by geographic origin, showing three major clades: Northern Population (NP), Southern Levant (SL), and *judaicum*. The Zavitan accession (TA11075), used as the reference genome, is indicated by a black dot (●). **h** Population structure of the WEW panel based on whole-genome sequencing markers (K = 2–5). Each vertical bar represents an accession, and colors indicate ancestry proportions. Accessions from Israel (excluding *judaicum*), Lebanon (LB), Syria, Palestine, and adjacent regions are grouped as SL, while NP includes accessions from southeastern Anatolia, Iran, and Iraq. The leftmost accession originates from Azerbaijan

(Supplementary Table S3) to investigate the genetic relationship between WEW subgroups (particularly *judaicum*) and cultivated emmer (*T. turgidum* subsp. *dicoccum*). The 31,277-SNP matrix, available via the Dryad link in the Data Availability section, was used to construct a phylogenetic tree highlighting the relationship between *judaicum*, cultivated, and other wild WEW groups.

Genotyping WGS panel

For WGS, PCR-free libraries using the TruSeq DNA PCR-FREE LT Sample Prep Kit (Illumina, Inc.) were generated followed by Illumina paired-end sequencing at Novogene (Novogene Co., Ltd., Beijing, China). Raw sequencing files were trimmed using fastp [18] and aligned to the WEW 'Zavitan' genome (WEW_v2.1) [19] using HISAT2 [20]. Variants were called with bcftools [21] and filtered by quality (≥ 30), read depth (≥ 20), allele frequency (0.01 < AF < 0.99), and missing data (≤ 0.2) [21]. Additional filtering was conducted for minor allele frequency (MAF < 0.05) and heterozygosity (removed > 10%). To reduce computational load while retaining representative genomic information, 5% of filtered variants were sampled per chromosome using GATK [22] and merged into a single VCF. Biallelic sites specific to the SL population were extracted from the filtered VCF using VCFtools [23] and used for GWAS, excluding the predominantly susceptible Northern population (NP) to focus on resistant accessions and minimize population structure effects.

Passport data curation

Allele matching was performed among WGS accessions using a ≥ 99% threshold to identify genetically identical (redundant) accessions [4, 24]. Passport data from gene banks were cross-checked against the USDA-ARS Germplasm Resources Information Network (GRIN) and Genesys (https://www.genesys-pgr.org/) to detect discrepancies. Any ambiguous passport information, particularly concerning the geographical coordinates of collection sites, was verified with the assistance of gene bank curators.

Population structure analysis

We explored the WEW population composition through phylogenetic clustering by generating a neighbor-joining (NJ) tree, principal component analysis (PCA), and population structure analysis as described [4, 24]. PCA was performed with eigenvalues/eigenvectors from the rrBlup A.mat in R [24, 25], plotting the first two eigenvectors with subgroup colors matching the NJ tree. Population structure analysis was done in R [26] using the Landscape and Ecological Association Studies (LEA) package as explained [27]. The numbers of population subgroups (K) were determined on the basis of the cross-entropy value. Ancestry proportions (Q matrix) were visualized using Pophelper [28].

Diversity and pairwise F_{ST}

We computed Nei's diversity index [29] and the total segregating alleles per subpopulation as previously described [4]. The diversity indices were computed for all accessions together and the subpopulations separately. The Weir and Cockerham F_{ST} [30], betas [31], $F_{ST,}$ and the Nei's pairwise F_{ST} [32] were computed between the subgroups using the R package 'hierfstat' [https://github.com/jgx65/hierfstat] [26].

Linkage disequilibrium, GWAS and comparative genomics

To examine linkage disequilibrium (LD) and its decay in the WEW panel, we selected a random, independent subset of 20,000 SNPs for each subpopulation (NP, *judaicum*, and Southern Levant). Pairwise LD (r^2) between all SNPs in each subset was calculated using VCFtools [23], and the physical distance (bp) between each SNP pair was recorded. SNP pairs were then binned by inter-marker distance into 100 kb intervals. Within each bin, mean r^2 values were computed to summarize LD decay as a function of physical distance. LD decay plots were generated by plotting mean r^2 against the midpoint of each distance bin using ggplot2 [33]. GWAS was performed using CMLM, BLINK, and FarmCPU models in GAPIT [34, 35] to cross-validate results and reduce model-specific bias.

We compared GWAS-identified loci with previously reported seedling rust resistance loci and candidate genes by mapping their genomic positions. Candidate genes with known orthologs were aligned to the Zavitan genome (v2.1) using BLASTn [36].

Results

WEW whole-genome sequencing panel, disease response and population analysis

The majority of WEW accessions originated from the regions of the Southern Levant (SL) and southeastern (SE) Anatolia, with only four accessions from Iran and 18 from Iraq (Fig. 1a, b Supplementary Table S1). Additionally, six accessions had no passport information. WEW accessions exhibited wide phenotypic variation in resistance to stem rust, leaf rust, and stripe rust at the seedling stage (Fig. 1d–f; Table 1 and Supplementary Table S1).

Genotyping and marker identification

The average sequencing depth across accessions was 9.5x (Supplementary Figure S1). After filtering, 68 million SNPs were retained, with a 5% subset containing 3,410,677 SNPs (Supplementary Table S4). SNP density

Table 1 Percentage of resistant or moderately resistant accessions per population group. Total accessions that were genetically grouped under Southern Levant (SL), Northern Population (NP) and *judaicum*

Disease	Pathogen races	Number and % Resistant (R)			Number and % Moderately Resistant (MR)		
		SL	NP	*judaicum*	SL	NP	*judaicum*
Stem rust	TTKSK	9 (5.4%)	0	0	15 (9%)	0	2 (5.7%)
	JRCQC	2 (1.2%)	0	0	8 (4.8%)	0	0
	TKTTF	5 (3%)	0	1 (2.8%)	8 (4.8%)	0	2 (5.7%)
	TTRTF	2 (1.2%)	0	0	5 (3%)	0	1 (2.9%)
	TTTTF	1 (0.6%)	0	0	11 (6.5%)	0	2 (5.7%)
Leaf rust	TBBGS	29 (17.4%)	3 (3.5%)	1 (2.8%)	3 (1.8%)	1 (1.2%)	2 (5.7%)
	BBBQD	8 (4.8%)	1 (1.2%)	3 (8.6%)	4 (2.4%)	1 (1.2%)	1 (2.9%)
	TFBGQ	3 (1.8%)	2 (2.4%)	0	3 (1.8%)	2 (2.4%)	0
	MFPSB	1 (0.6%)	1 (1.2%)	0	5 (3%)	3 (3.5%)	0
	TNBGJ	4 (2.4%)	2 (2.4%)	1 (2.8%)	9 (5.4%)	1 (1.2%)	1 (2.8%)
Stripe rust	PSTv-221	47 (28.1%)	0	4 (11.4%)	37 (22.2%)	1 (1.2%)	6 (17.4%)
	PSTv14	34 (20.4%)	2 (2.4%)	0	51 (30.5%)	10 (11.8%)	6 (17.1%)
	PSTv-143	38 (22.8%)	0	5 (14.3%)	40 (24%)	11 (13%)	9 (25.7%)
	PSTv-5006	53 (31.7%)	0	9 (25.7%)	31 (18.6%)	14 (16.5%)	8 (22.8%)
	PSTv-37	55 (33%)	5 (5.9%)	6 (17.4%)	55 (33%)	14 (16.5%)	13 (37.1%)

varied across the 14 chromosomes, with higher variant density in centromeric and peri-centromeric regions (Supplementary Figure S2), which can be related to more extensive diversity of older transposable elements in pericentric regions as well as lack of read mapping due to divergence from the reference (Zavitan) in highly diverse telomeric regions. All chromosomes had > 200,000 SNPs (Supplementary Table S4), ensuring sufficient marker coverage for downstream analyses. SNP matrices are available in the Dryad repository (see Data Availability).

Passport data curation

Allele matching revealed five groups of redundant WEW accessions (Supplementary Table S5). Most of these redundant accessions (TA117 and TA1459; TA11202, TA11203 and TA119; TA131, TA132 and TA133; TA134 and TA135) were collected in nearby locations (Supplementary Table S1), particularly from the Golan Heights and surrounding regions. We also standardized "collection site" information between the gene bank and the USDA GRIN database to account for historical shifts in geographic terminology. The corrected WEW passport data are provided in Supplementary Table S6.

Phylogenetic tree and PCA

The unrooted NJ phylogenetic tree revealed three major WEW clades (Fig. 1g). Notably, a group of accessions near the Sea of Galilee formed a distinct clade, showing strong genetic differentiation even within the same region. These accessions belong to the wide-spiked subgroup *judaicum* (n = 35 accessions) based on comparisons with previous spike morphology data [37, 38]. Accessions from southeastern Turkey, Iran, and Iraq formed the Northern Population (NP, n = 85), while southern Levant accessions clustered into a major SL subgroup (n = 167), including a subclade from Lebanon and Syria (Fig. 1g). These genetically distinct subgroups correspond to the NP, SL, and *judaicum*, consistent with previous reports [17, 39, 40]. Four accessions (TA120, TA1468, TA11175, TA11193) clustered at the base of the SL clade, near the NP–*judaicum* split, while two Syrian accessions (TA11208, TA11218) grouped with northern Lebanon and southern Syria accessions. Interestingly, two accessions (TA11212 and TA1213) from Lebanon originating from the An Nabatiyah and Anti-Lebanon regions, respectively, and another accession, TA11233, from the SL group, formed a subclade near the base of the NP clade along with some other accessions lacking passport information. Together, these accessions appear to bridge the NP and SL subgroups (Fig. 1g). PCA results mirrored the phylogeny, with *judaicum* forming a distinct subgroup within SL, clearly separated from neighboring accessions (Fig. 1g, Supplementary Figure S3).

Population structure

Population structure analysis confirmed differentiation of the WEW collection into subgroups NP, SL, and *judaicum*, as well as admixtures, consistent with the phylogeny and PCA. At K = 2, only *judaicum* was separated, while NP and SL were distinguished at K ≥ 3 (Fig. 1h). Cross-entropy analysis supported K = 4 as an optimal statistical model (Supplementary Figure S4), at which we observed some population differentiation within the Southern Levant consisting of accessions originating from Lebanon. However, the differentiation observed at K = 3 corresponded directly to the three major clades identified by phylogenetic and PCA analyses. Four accessions that did

not cluster within NP, SL, or *judaicum* were classified as admixed (Fig. 1g, h).

To assess the relationship with domesticated emmer, 31,277 GBS-derived SNPs were analyzed. Phylogenetic clustering revealed domesticated emmer is more closely related to accessions in the NP (Supplementary Figure S5), indicating that accessions from the SL and *judaicum* are not immediate ancestors.

Diversity and F_{ST}

The SL population showed the highest Nei's diversity index (0.17) and number of segregating alleles, followed by NP (0.15) and *judaicum* (0.06) (Supplementary Table S7). Pairwise F_{ST} analyses (Weir and Cockerham, beta, and Nei's) consistently indicated *judaicum* as the most differentiated subgroup. The lowest divergence was between NP and SL (Nei's F_{ST} = 0.05), while the highest was between *judaicum* and NP (Nei's F_{ST} = 0.204) (Supplementary Table S8). Thus, *judaicum* represents the most genetically distinct WEW subgroup compared to the NP and SL populations.

Genetic resources for disease resistance in WEW panel

Across all 15 rust races, WEW accessions exhibited a wide range of seedling-stage responses (Fig. 2a), from resistant (R) to susceptible (S) (Supplementary Table S9–S10). Stem rust resistance was relatively rare, with only 3–6% of accessions showing resistant or moderately resistant reactions. Accessions with resistance to TTKSK (R = 3%, MR = 6%) and TKTTF (R = 2%, MR = 3%) may be particularly valuable in breeding programs. Leaf rust resistance was more common, with up to 12% of accessions resistant to race TBBGS and 4–6% to other races. Notably, accession TA11156 was fully resistant (infection type = 0) to all five leaf rust races, representing an exceptional genetic resource, although it was not genotyped. Stripe rust resistance was the most frequent, with up to 23% of accessions resistant to PSTv-37 and 22% to PSTv-5006, and 15–29% showing moderate resistance across races. Seventeen accessions were fully resistant to all five stripe rust races (Supplementary Table S11). Four accessions showed resistance to three or more leaf rust races, and five were fully resistant to two or more stem rust races (Supplementary Table S11). At least four accessions, including TA1041 and TA1047, were fully resistant to all five stripe rust races and at least one race of another pathogen. Overall, these results highlight WEW accessions as exceptional genetic resources for rust resistance.

Distribution of resistance across geography

Across all three rust diseases, the SL subpopulation consistently contributed a higher proportion of resistant or moderately resistant accessions compared to the NP and *judaicum* subpopulations (Table 1; Figs. 2, 3, 4 and 5, Supplementary Table S9). The responses to the diseases also varied among subpopulations for each pathogen race (Fig. 2a).

Geographical distributions of stem rust resistance

Most stem rust-resistant accessions originated from the SL subpopulation, with only limited resistance observed in *judaicum* and none in the NP subpopulation (Table 1; Figs. 2a-c and 3). Within SL, the highest proportion of resistant accessions (5.4%) was detected against race TTKSK, while the lowest (0.6%) occurred against TTTTF. Moderately resistant accessions were also most frequent in SL (9% to 6.5%) and *judaicum* (up to 5.7% against TTKSK and TTTTF), whereas NP showed no resistance or moderate resistance to any races of the stem rust pathogen race (Table 1). In *judaicum*, the highest number of resistant (R = 2.8%) and moderately resistant (MR = 5.7%) accessions was observed against TKTTF (Fig. 3).

Geographical distributions of leaf rust resistance

Similar to stem rust, most leaf rust-resistant accessions originated from the SL subpopulation (Table 1; Fig. 4). The highest proportion of resistant accessions in SL (17.4%) occurred against TBBGS, while the lowest (0.6%) was found against MFPSB. Moderate resistance in SL ranged from 1.8% to 5.4%, with the highest observed against TNBGJ. In NP, resistant accessions ranged from 1.2% to 3.5%, and moderately resistant ones from 1.2% to 3.5%. In the *judaicum* group, resistance reached up to 8.6% (race BBBQD), while moderate resistance peaked at 5.7% for TBBGS.

Geographical distributions of stripe rust resistance

Stripe rust resistance was most prevalent in the SL subpopulation (Table 1, supplementary Table S9, Fig. 5). The highest percentage of resistant accessions in SL (33%) was observed against race PSTv-37, while the lowest (20.4%) occurred against PSTv-14. Moderate resistance in SL ranged from 18.6% to 33%, also peaking against PSTv-37. The NP subgroup showed limited resistance (0–5.9%) and moderate resistance (1.2–16.5%), with the highest levels for PSTv-37. In *judaicum*, resistance ranged from 0% to 25.7% and moderate resistance from 17.1% to 37.1%, both peaking against PSTv-37 (Fig. 5).

Genome-Wide Association Study (GWAS)

Linkage disequilibrium

In each subpopulation (SL: 167, NP: 85, and *judaicum* 35), the linkage decay was rapid over the first 250 kb (Supplementary Figure S6) with the pattern varying slightly among the subpopulations. Specifically, in the *judaicum* subpopulation, the mean r^2 dropped from 0.8 to 0.4 (half) over this interval, whereas in the SL and NP,

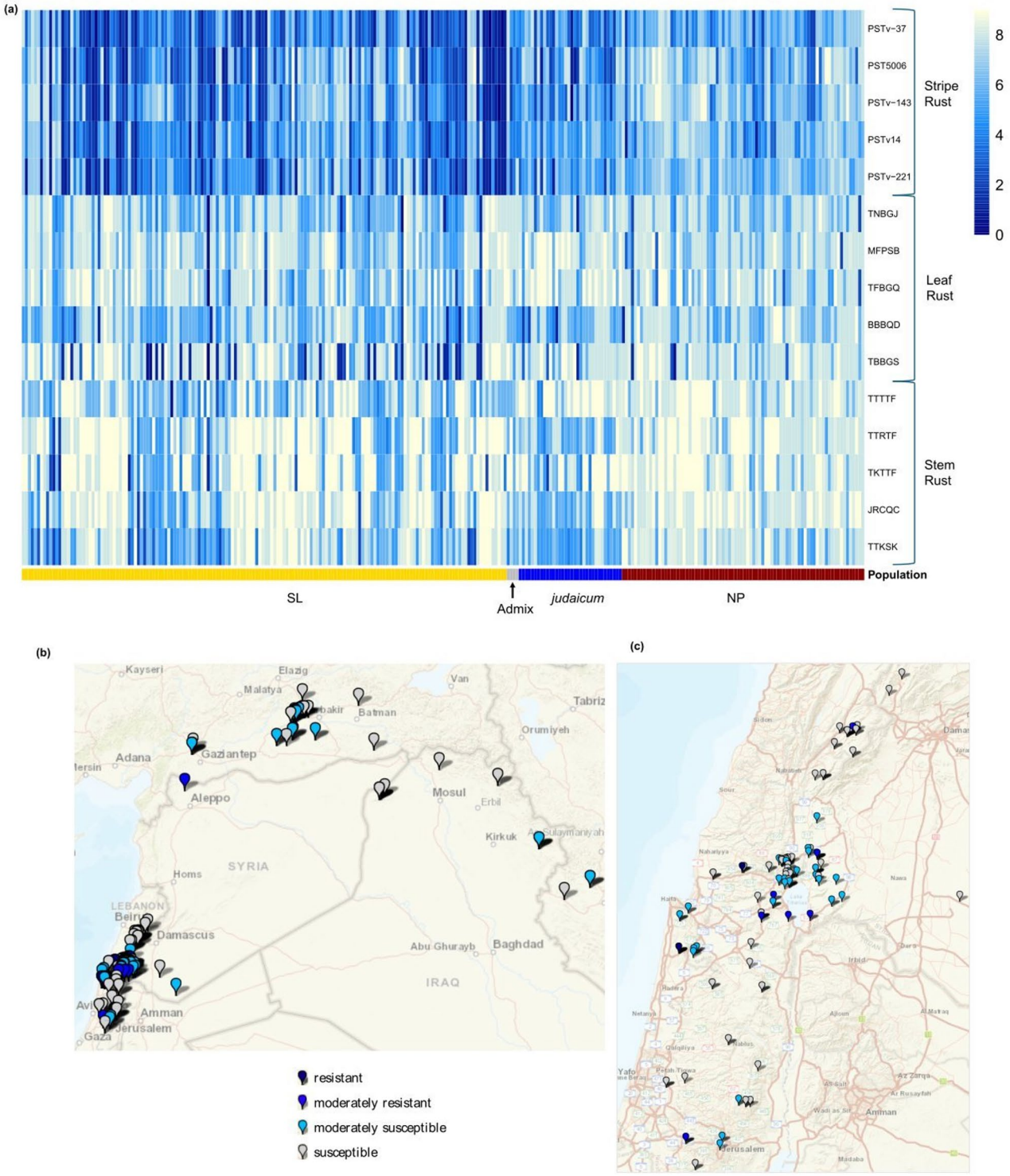

Fig. 2 Distribution of rust-resistant accessions across population subgroups. **a** Accessions from the Southern Levant (SL), Northern Population (NP), *judaicum*, and admixed subgroups are shown with their resistance levels, ranging from highly resistant (dark blue; score 0) to susceptible (white; score 9). Each vertical bar represents an individual accession. Resistance responses are displayed in three panels corresponding to stem rust, leaf rust, and stripe rust. **b** Phenotypic responses of all accessions evaluated against *Puccinia graminis* f. sp. *tritici* race TTKSK at the seedling stage. **c** Enlarged view of the distribution of TTKSK resistance within the SL and *judaicum* subgroups

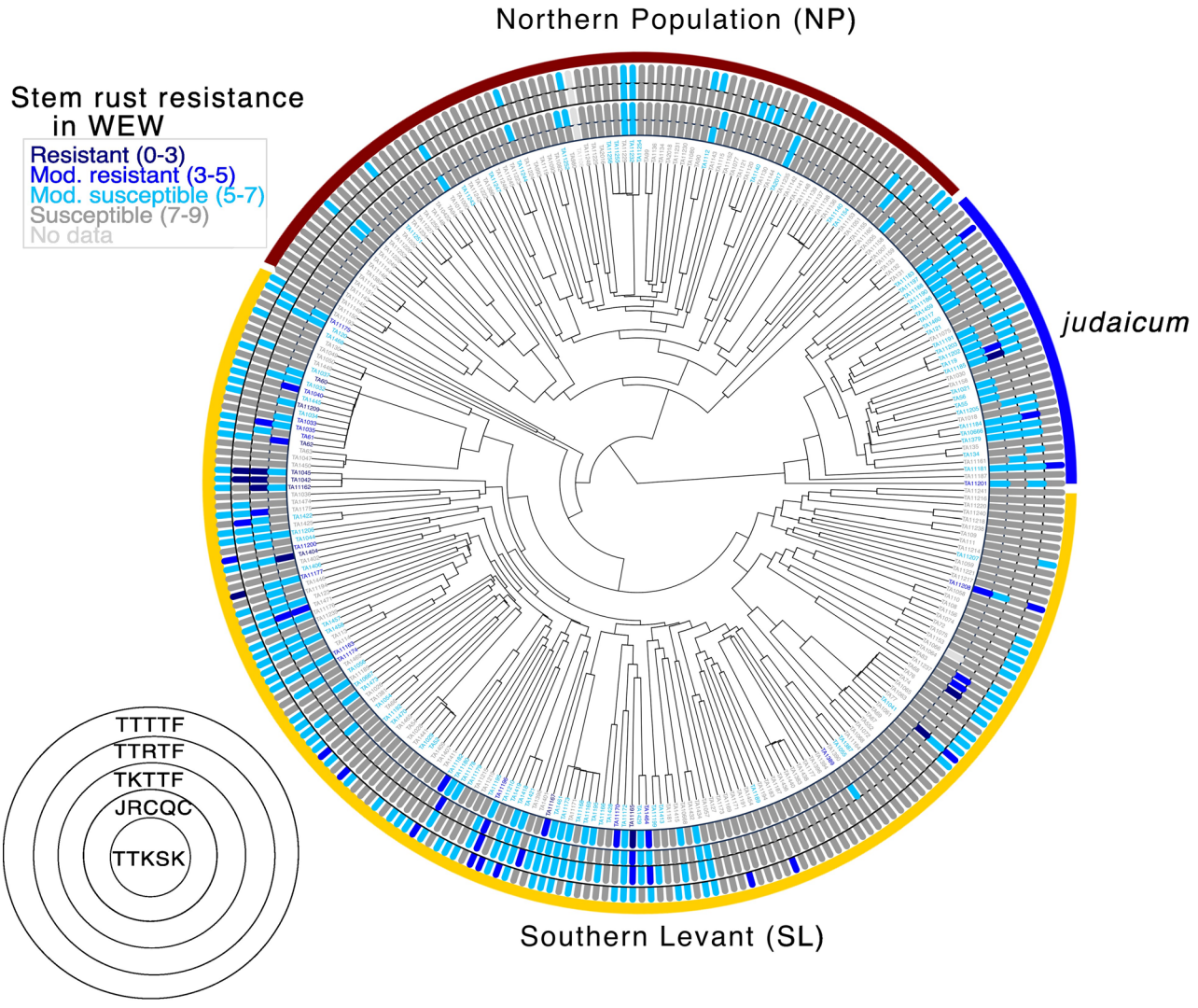

Fig. 3 Neighbor-joining (NJ) tree of clustering of wild emmer wheat accessions with geographic origins and levels of resistance to five *P. g.* f. sp. *tritici* races at the seedling stage. The TA designations of accessions are shown at the outer ends of the tree branches, representing resistance levels to race TTKSK. The four outer bands of segments surrounding the branch tips indicate general rust reactions: resistant (navy), moderately resistant (blue), moderately susceptible (deep sky blue), and susceptible (medium gray), with the corresponding colors matching the legend in the top left. The outer solid band indicates the subgroups—southern Levant (gold), northern population (dark red), and *judaicum* (blue)

the mean r^2 dropped from 0.5 to 0.25 and from 0.7 to 0.35, respectively (Supplementary Figure S6). However, we still observed extended LD with $r^2 > 0.2$ at 40 Mb in the *judaicum* and at 100 Mb in the Northern Population.

GWAS for stem rust resistance

GWAS was performed on the SL population comprising 167 accessions. Across five *P. g.* f. sp. *tritici* races, 27 significant loci were detected (Supplementary Table S12). The strongest signal was on 1BS (~ 50–97 Mb), which explained up to 73.5% of the phenotypic variance (PVE) for TTKSK and was consistently detected across GWAS models (Supplementary Table S12, Fig. 6) This likely reflects a major-effect resistance allele segregating in this population. Additional loci for TTKSK were found on 3B at 194 Mb and 380 Mb. Many associations appear novel, though a few have been previously reported [41]. For JRCQC, the same 1BS region was most significant at 72 Mb, with additional loci on 3AS and 7AL (Supplementary Table S12).

For TKTTF, the 1BS peak remained highly significant, along with loci on 2BL, 3BS, 5AL, 6BL, and 7AL. TTRTF resistance was associated with loci on 3AL and 5AL, whereas TTTTF resistance involved loci on 1AL, 1BS, 2AS, 2AL, 4BL, 5AS, 5BL, and 6AL. Overall, 1BS was repeatedly detected across multiple races, while most other loci showed race-specific effects, highlighting the complex genetic architecture of stem rust resistance in WEW.

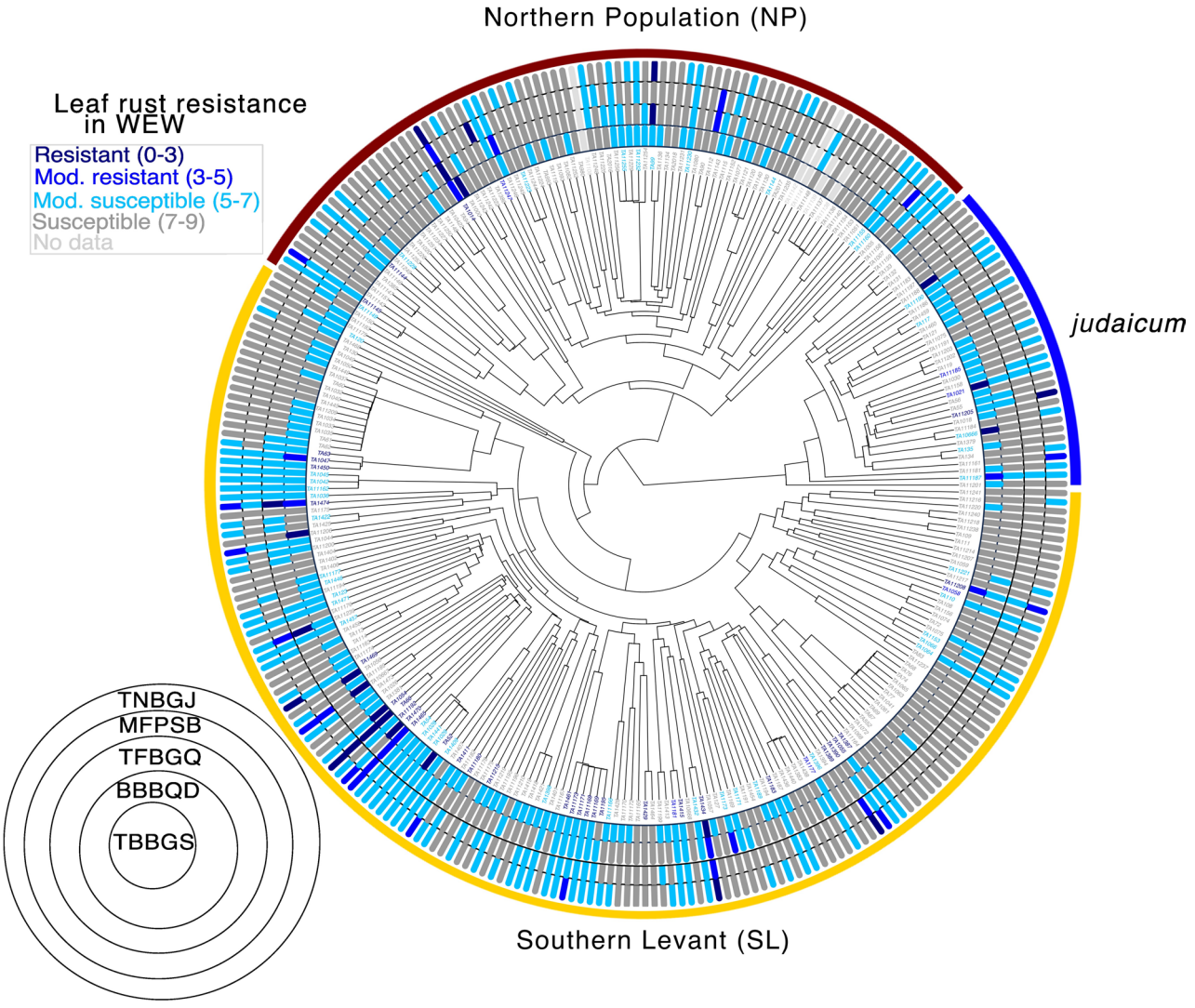

Fig. 4 Neighbor-joining (NJ) tree of wild emmer wheat accessions with geographic origins and levels of resistance to five *P. triticina* races at the seedling stage. The resistance levels were differentiated based on disease scores, with corresponding colors on the tree matching the legend color at the top left. The innermost tree features labels of accessions as TA#, while the outer tree branches are represented by colors only. The outer colored circle's segments within the NJ tree delineate subgroups: SL, NP, and *judaicum*

GWAS for the leaf rust

Across five *P. triticina* races, GWAS identified 26 significant loci associated with seedling-stage resistance (Supplementary Table S13). The most prominent association was observed for BBBQD, with a locus on 3B explaining 55.7% of the PVE. Major loci for TFBGQ were detected on 3B and 6B, with PVE values up to 30.8%, while MFPSB resistance involved multiple moderate-effect loci, particularly on 2A and 2B (up to ~15% PVE). TNBGJ resistance was largely associated with loci on 2B (28.4% PVE) and 1B (12.4% PVE), along with smaller-effect loci on 4A, 4B, and 6A. TBBGS exhibited associations across several chromosomes (1B, 2A, 3A, 4A, 4B, 5B, 7A), though most loci had modest effects (< 5% PVE).

GWAS for stripe rust resistance

Genome-wide association analysis for five stripe rust races identified a total of 41 significant loci, ranging from 5 to 12 loci per race (Supplementary Table S14). The loci were distributed across most chromosomes, with several explaining substantial phenotypic variation (up to 22.2% PVE). Only 1B_137686692 was repeatedly detected across two races (PSTv-14 and PSTv-5006), indicating that most stripe rust resistance loci in WEW are race-specific. Major loci had moderate to high effect sizes, and MAF varied widely, reflecting both common and rare resistance alleles in the population (Supplementary Table S14).

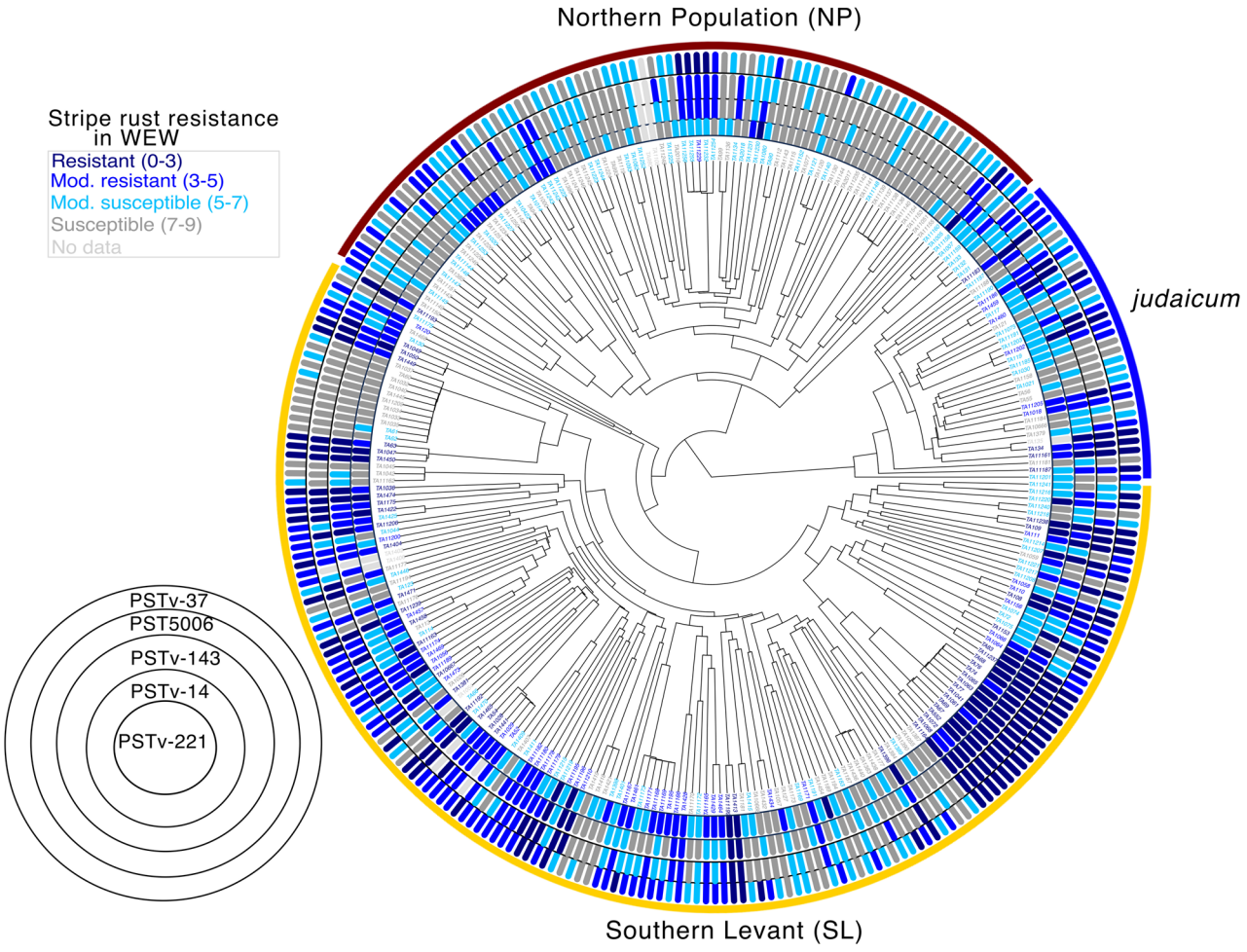

Fig. 5 Neighbor-joining (NJ) tree of wild emmer wheat accessions with geographic origins and levels of resistance to five *P. s.* f. sp. *tritici* races at the seedling stage. The resistance levels were differentiated based on disease scores, with corresponding colors on the tree matching the legend color at the top left. The innermost tree features labels of accessions as TA#, while the outer tree branches are represented by colors only. The outer colored circle's segments within the NJ tree delineate subgroups: NP, SL and *judaicum*

Discussion

Population structure and the *judaicum* subgroup

The distinct genetic separation of the *judaicum* subgroup from the rest of the SL population is a notable finding in this study (Fig. 1g, h and Supplementary Figure S3). The clustering of northern Syrian accessions with those from Lebanon and southern Syria likely reflects dispersal of WEW along the Mediterranean coast, consistent with southeastern Anatolia and northern Syria being centers of emmer domestication [42, 43]. Observed admixture in four accessions indicates gene flow across broader geographic regions (Fig. 1g, h).

Some authors have treated *judaicum* as a separate subspecies of *T. turgidum* [37], while others considered it a race, contrasting it morphologically with the *horanum* race of the SL population [38]. Blumler (1998) suggested that the origin of *judaicum* stems from the hybridization of wild emmer and durum wheat. Our analyses indicate that *judaicum* is neither a direct ancestor of domesticated emmer nor a feral subgroup (Supplementary Figure S5), though further investigation is needed to fully characterize its evolutionary history [40, 44].

Geographic variation in rust resistance

Rust resistance patterns differed among WEW subpopulations. The SL subgroup exhibited the broadest spectrum of resistance, making it a particularly valuable source of resistance alleles for breeding. The subgroup *judaicum* showed intermediate resistance, while NP lacked stem rust resistance, although it retained resistance to some leaf rust races and all stripe rust races, indicating the presence of some R genes (Table 1, Supplementary Table S1, Figs. 4 and 5) [41]. Overall, SL was the only subgroup with accessions resistant to all 15 rust races, although its resistance to stem and leaf rust was proportionally lower than to stripe rust. This pattern aligns with previous observations; for example, *Yr15* and

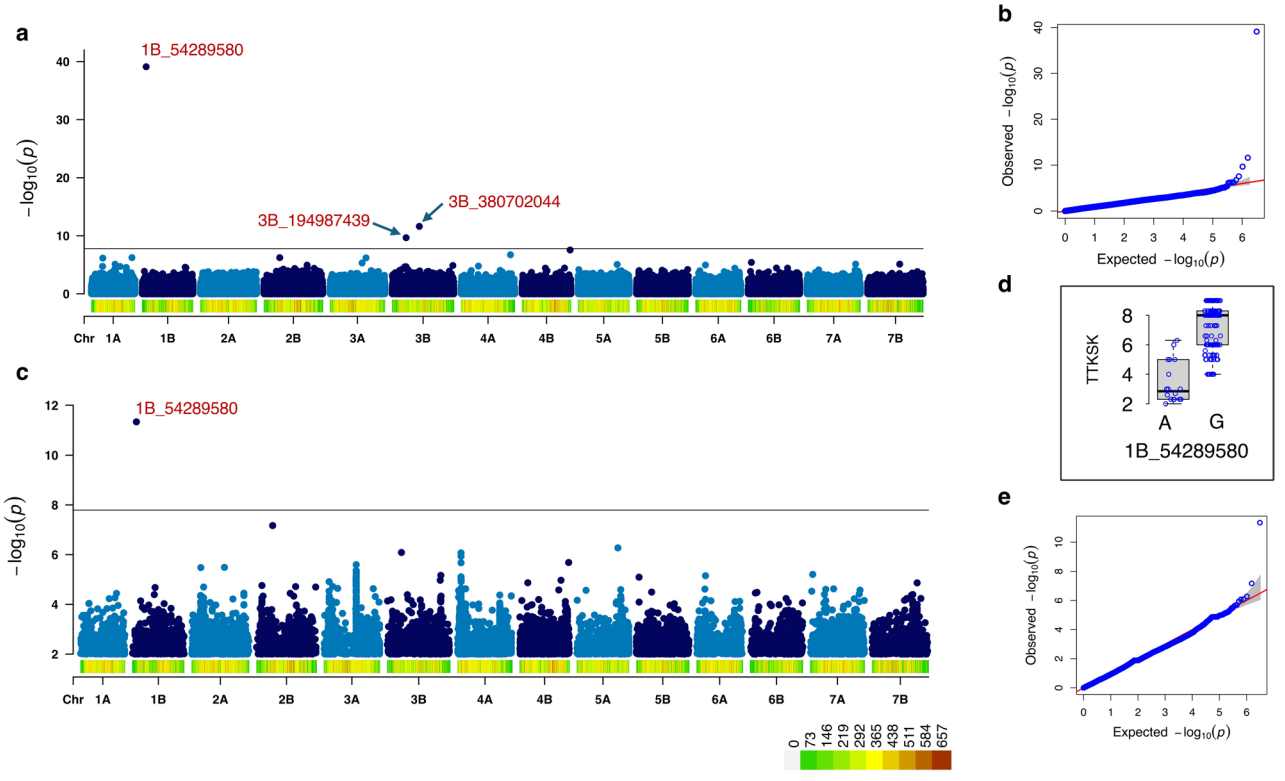

Fig. 6 GWAS of stem rust resistance to race TTKSK of *P. g.* f. sp. *tritici*. **a** Manhattan plot for race TTKSK resistance with FarmCPU model; **b** QQ-plot (right) showing the deviation of the observed p-values from the null hypothesis for the FarmCPU method; **c** TTKSK Manhattan plot with Blink method; **d** the phenotype distribution for the alleles of the most significant loci at 54,289,580 on chromosome 1BS; **e** the p-values QQ plot for the Blink method. The horizontal line in both Manhattan plots represents the Bonferroni-adjusted p-value set at 0.05 [p_{adj} = 0.05]. Candidate loci were annotated with their marker names. GWAS was performed using 3,085,492 biallelic SNPs from the SL subgroup

Yr36, cloned from southern populations, are absent in NP accessions [12, 45].

Seedling stage disease resistance is mostly quantitative

Seedling-stage responses in WEW ranged from highly resistant to highly susceptible (Supplementary Table S9). The number of loci associated with resistance varied by race, from one (leaf rust race BBBQD) to twelve (stripe rust race PSTv-14). Multiple QTL were detected across races, consistent with prior reports in cultivated and wild wheat. For example, fifteen QTL for BBBQD were reported in cultivated emmer [46], while Tene et al. (2022) and Megerssa et al. (2021) reported minor QTL for stripe rust and multiple loci for stem rust resistance in WEW and durum wheat. This study also confirms the polygenic nature of rust resistance in WEW, with both major- and minor-effect loci contributing to race-specific resistance.

Disease-resistant accessions as genetic resources

Several WEW accessions exhibited broad-spectrum resistance, highlighting their value as genetic resources (Supplementary Table S11). Some stripe rust races, such as Pst-221 and Pst-143, had not been previously tested on WEW, and reports on leaf rust resistance remain limited. Notable examples include TA66, which was highly resistant to all leaf rust races (Supplementary Table S9); TA11204, resistant or moderately resistant to 10 of 15 races; and TA1041, TA1047, and TA11196, which collectively provide promising germplasms for novel genes for breeding broad-spectrum resistance. These accessions represent ideal candidates for introgression into elite wheat lines to develop cultivars with durable rust resistance.

High prevalence of stripe rust resistance in SL

Approximately 50% of SL accessions were resistant or moderately resistant to all five stripe rust races (Table 1; Figs. 2a and 5), confirming previous observations of high resistance in this subgroup compared to NP [17]. While resistance to leaf and stem rust was lower across all subgroups, the abundance of stripe rust-resistant lines in SL underscores its value as a source of alleles for breeding. Leveraging this diversity through gene pyramiding could accelerate the development of cultivars with durable rust resistance.

Known and novel resistance loci with a 1BS as a resistance hotspot

GWAS identified 27 loci for stem rust resistance, of which 26 appear to be novel (Supplementary Table S12). A highly significant locus on 1BS (1B_54289580) associated with resistance to race TTKSK was also reported previously in WEW [41] and in durum wheat [47]. The *trichome birefringence-like* (*TBL*) ortholog aligned to this same region in the Zavitan reference genome (Supplementary Table S15). The 1BS interval (~ 50–97 Mb) contained multiple resistance loci to different races, including at 72 Mb (JRCQC, TTKSK), 56 Mb and 96 Mb (TKTTF), and 99 and 102 Mb (TTTTF). This region was examined for LD structure with low LD observed between some of the associated loci, suggesting multiple R-genes in this region (Supplementary Figure S7). Some loci were located near known *Sr* genes on Zavitan. The *Sr22* ortholog from *T. monococcum* aligned at 7A (700 Mb), while a locus for race JRCQC was mapped at 722 Mb. A locus for TTTTF on 5BL corresponded to the *Sr49* region identified previously [48]. Likewise, *Sr13* and *Sr8155B1* orthologs from durum wheat aligned at 628 Mb and 467 Mb, respectively, on 6AL, and a nearby TTTTF locus at 574 Mb may represent related alleles. The *Sr9B* coding sequence aligned with 99% identity at 2BL (699 Mb), close to the TKTTF locus detected at 714 Mb (Supplementary Table S15).

Nearly all QTL detected for leaf rust were novel. A locus on 7BS (7B_68229888) for race MFPSB may correspond to a previously reported 7BS QTL in durum wheat for race BBG/BN [49]. Some loci colocalized with known *Lr* gene regions on the Zavitan genome, including *Lr10* (4A_751 Mb; QTL at 748 Mb for TBBGS), *Lr67* (4BL_515 Mb; QTL at 558 Mb), and *Lr72* (7BS_68 Mb, MFPSB) [50]. The 1BS region also contributed to leaf rust resistance, with loci at 99 Mb for TBBGS and 7 and 55 Mb for TNBGJ, suggesting that this region may serve as a shared resistance hotspot across rust pathogens.

Of 41 loci associated with stripe rust resistance, only four overlapped with previously reported regions:1BS (PSTv-14), 4B (PSTv-5006), 1A and 1B (PSTv-37), while the remainder were novel. Several loci colocalized with known *Yr* gene regions, including *Yr15* (1BS_97.9 Mb; 93% identity) and *Yr36* (6B_149 Mb; 98% identity) [51]. Although *Yr36* is typically associated with adult plant resistance, it may also act at the seedling stage when combined with *Yr18* or *Yr28*. Additional interesting pairs of GWAS loci and known genes included an *ethylene-responsive transcription factor 3-like* gene on 7A_638642386 (PSTv-14) and a *WRKY* transcription factor near 137 Mb (PSTv-14, PSTv-5006), both previously associated in rust resistance [52, 53].

Cloned genes from SL subgroup

Many cloned R genes originate from the SL subgroup, reflecting its high abundance of resistant accessions. Notable examples include H52 (Mount Hermon), which carries *YrH52* [54]; G25 (TA1474, Rosh Pinna), harboring *Yr15* [55] and *PmG25* [56]; G-305-M, carrying *PmG3M*, effective against 41 isolates from multiple wheat species [57–59]; and *Pm36*, present in only a few SL lines [11]. Our phenotyping confirmed that TA1474 was resistant or moderately resistant to four leaf rust races and all stripe rust races (Supplementary Table S9), supporting the reliability of our screening. These findings emphasize the importance of assessing R gene diversity in SL relative to NP and *judaicum*.

Promising target loci and candidate genes

GWAS identified both previously characterized and novel loci associated with rust resistance (Supplementary Tables S12–S15). A notable candidate is *Trichome birefringence-like 10* (*TBL10*) on 1BS, which aligns with a multi-rust resistance hotspot (~ 50–97 Mb). In Arabidopsis, *TBL* genes contribute to secondary cell wall formation through cellulose synthesis and pectic polymer esterification [60]. Similarly, in the barley (*Hordeum vulgare*)–*P. graminis f.* sp. *tritici* pathosystem, Sharma et al. (2018) reported that three of seven *Rrr1* candidate genes belong to the TBL family, which can function as positive or negative regulators depending on the interaction [61]. This 1BS region also contains loci near known *Sr* genes, including *Sr22*, *Sr13*, *Lr10-like*, and *Yr15*, making it a prime target for functional validation and introgression into breeding programs. The presence of both novel and known resistance loci underscores the potential of WEW as a source of alleles for durable, broad-spectrum rust resistance.

Conclusions

We analyzed a large whole-genome-sequenced panel of WEW to investigate population structure, genetic diversity, and rust resistance loci. Three distinct subgroups (SL, NP, and *judaicum*) highlight evolutionary differentiation, with SL harboring the greatest diversity of resistance alleles. Several accessions exhibited broad-spectrum resistance to multiple rust races, representing a valuable genetic resource. GWAS identified both known and novel loci, including a major hotspot on chromosome 1BS associated with multiple rust pathogens. These findings provide a foundation for functional studies and the targeted use of WEW germplasm in breeding wheat varieties with durable, broad-spectrum rust resistance.

Abbreviations

GBS	Genotyping-by-sequencing
GWAS	Genome-wide association study
LD	Linkage disequilibrium

NP	Northern population
QTL	Quantitative trait loci
SE	Southeastern
SL	Southern Levant
WEW	Wild emmer wheat
WGS	Whole-genome sequencing

Supplementary Information

The online version contains supplementary material available at https://doi.org/10.1186/s12864-026-12751-6.

Supplementary Material 1.

Supplementary Material 2.

Acknowledgements

We thank the Wheat Genetics Resource Center (WGRC) at Kansas State University and the University of Bologna, Bologna, Italy for providing germplasm. For initial germplasm collections of some WEW lines, we acknowledge the National BioResource Project (NBRP) in Komugi, Kyoto, Japan and Hakan Özkan Çukurova University, Adana, Turkey). Computational analyses were performed using the Beocat supercomputer at Kansas State University and the Supercomputing Core Laboratory at KAUST in Thuwal, Saudi Arabia.

Authors' contributions

B.J.S., J.P., and B.W. conceptualized the study, secured grants, and provided ongoing guidance. J.R., E.M., A.B., R.T, and H.O. maintained germplasm and distributed seed. J.R. and H.S. curated germplasm passport information. P.O. conducted phenotyping and analyzed phenotype data. L.A. conducted sequence data curation, genotyping, and population analysis. A.D. and H.S. assisted in population analysis and provided an updated Zavitan genome annotation. L.A. and P.O., with the assistance of B.J.S. and J.P., prepared the initial draft of the manuscript. L.A., B.J.S., J.P., and B.W. revised the manuscript, and all authors read and reviewed the final version.

Funding

This research was supported by the National Institute of Food and Agriculture, U.S. Department of Agriculture, under award number 2020-67013-30871 to the 2Blades Foundation, the Lieberman-Okinow Endowment at the University of Minnesota to B.S., and baseline funds from King Abdullah University of Science and Technology to B.W and J.P.

Data availability

A variant call format (VCF) file, hapmap file with the SNP matrix generated with WGS as well as GBS data, and Linux script and statistical codes used in the study, were deposited in the Dryad public repository under https://doi.org/10.5061/dryad.zcrjdfnmb. The WGS data of the WEW panel has been deposited in the NCBI public repository sequence read archive (SRA) under the BioProject accession # PRJNA1007489.

Declarations

Ethics approval and consent to participate

Not applicable.

Consent for publication

Not applicable.

Competing interests

The authors declare no competing interests.

Author details

[1]Plant Science Program, Biological and Environmental Science and Engineering Division, King Abdullah University of Science and Technology (KAUST), Thuwal 23955, Saudi Arabia
[2]Wheat Genetics Resource Center, Department of Plant Pathology, Kansas State University, Manhattan, KS 66502, USA
[3]Department of Plant Pathology, University of Minnesota, Saint Paul, MN 55108, USA
[4]Department of Evolutionary and Environmental Biology, University of Haifa, Haifa 3498838, Israel
[5]Department of Agricultural and Food Sciences, Università di Bologna, Bologna, Italy
[6]Council for Agricultural Research and Economics-Research Centre for Genomics and Bioinformatics, Fiorenzuola d'Arda, Italy
[7]Council for Agricultural Research and Economics-Centre for Animal Production and Aquaculture (CREA-ZA), Viale Piacenza 29, Lodi 26900, Italy
[8]Department of Field Crops, Faculty of Agriculture, University of Çukurova, Adana 01250, Turkey
[9]State Key Laboratory of Wheat Improvement, College of Agronomy, Shandong Agricultural University, Tai'an, Shandong, China

Received: 27 October 2025 / Accepted: 11 March 2026
Published online: 16 March 2026

References

1. Singh RP, Hodson DP, Huerta-Espino J, Jin Y, Bhavani S, Njau P, Herrera-Foessel S, Singh PK, Singh S, Govindan V. The emergence of Ug99 races of the stem rust fungus is a threat to world wheat production. Annu Rev Phytopathol. 2011;49:465–81.
2. Chai Y, Pardey PG, Hurley TM, Senay SD, Beddow JM. A Probabilistic Bio-Economic Assessment of the Global Consequences of Wheat Leaf Rust. Phytopathology®. 2020;110(12):1886–96.
3. Beddow JM, Pardey PG, Chai Y, Hurley TM, Kriticos DJ, Braun H-J, Park RF, Cuddy WS, Yonow T. Research investment implications of shifts in the global geography of wheat stripe rust. Nat Plants. 2015;1(10):15132.
4. Adhikari L, Raupp J, Wu S, Koo D-H, Friebe B, Poland J. Genomic characterization and gene bank curation of Aegilops: the wild relatives of wheat. Front Plant Sci. 2023;14:1268370.
5. Balla MY, Gorafi YSA, Kamal NM, Abdalla MGA, Tahir ISA, Tsujimoto H. Harnessing the diversity of wild emmer wheat for genetic improvement of durum wheat. Theor Appl Genet. 2022;135(5):1671–84.
6. Ahmed HI, Heuberger M, Schoen A, Koo D-H, Quiroz-Chavez J, Adhikari L, Raupp J, Cauet S, Rodde N, Cravero C, et al. Einkorn genomics sheds light on history of the oldest domesticated wheat. Nature. 2023;620(7975):830–8.
7. Oliveira HR, Jacocks L, Czajkowska BI, Kennedy SL, Brown TA. Multiregional origins of the domesticated tetraploid wheats. PLoS ONE. 2020;15(1):e0227148.
8. Özkan H, Willcox G, Graner A, Salamini F, Kilian B. Geographic distribution and domestication of wild emmer wheat (*Triticum dicoccoides*). Genet Resour Crop Evol. 2011;58(1):11–53.
9. Li M, Dong L, Li B, Wang Z, Xie J, Qiu D, Li Y, Shi W, Yang L, Wu Q, et al. A CNL protein in wild emmer wheat confers powdery mildew resistance. New Phytol. 2020;228(3):1027–37.
10. Gioia T, Nagel KA, Beleggia R, Fragasso M, Ficco DBM, Pieruschka R, De Vita P, Fiorani F, Papa R. Impact of domestication on the phenotypic architecture of durum wheat under contrasting nitrogen fertilization. J Exp Bot. 2015;66(18):5519–30.
11. Li M, Zhang H, Xiao H, Zhu K, Shi W, Zhang D, Wang Y, Yang L, Wu Q, Xie J, et al. A membrane associated tandem kinase from wild emmer wheat confers broad-spectrum resistance to powdery mildew. Nat Commun. 2024;15(1):3124.
12. Klymiuk V, Yaniv E, Huang L, Raats D, Fatiukha A, Chen S, Feng L, Frenkel Z, Krugman T, Lidzbarsky G, et al. Cloning of the wheat Yr15 resistance gene sheds light on the plant tandem kinase-pseudokinase family. Nat Commun. 2018;9(1):3735.
13. Klymiuk V, Chawla HS, Wiebe K, Ens J, Fatiukha A, Govta L, Fahima T, Pozniak CJ. Discovery of stripe rust resistance with incomplete dominance in wild emmer wheat using bulked segregant analysis sequencing. Commun Biol. 2022;5(1):826.
14. Fu D, Uauy C, Distelfeld A, Blechl A, Epstein L, Chen X, Sela H, Fahima T, Dubcovsky J. A Kinase-START Gene Confers Temperature-Dependent Resistance to Wheat Stripe Rust. Science. 2009;323(5919):1357–60.
15. Zhang H, Ren Z, Hu Y, Wang C, Ji W. Characterization of wheat stripe rust resistance genes in Shaanmai 139. Acta Agron Sin. 2010;36(1):109–14.
16. Bai D, Knott DR. Genetic studies of leaf and stem rust resistance in six accessions of *Triticum turgidum* var. *dicoccoides*. *Genome* 1994, 37(3):405–409.

17. Tene M, Adhikari E, Cobo N, Jordan KW, Matny O, del Blanco IA, Roter J, Ezrati S, Govta L, Manisterski J, et al. GWAS for Stripe Rust Resistance in Wild Emmer Wheat (*Triticum dicoccoides)* Population: Obstacles and Solutions. Crops. 2022;2(1):42–61.
18. Chen S, Zhou Y, Chen Y, Gu J. fastp: an ultra-fast all-in-one FASTQ preprocessor. Bioinformatics. 2018;34(17):i884–90.
19. Zhu T, Wang L, Rodriguez JC, Deal KR, Avni R, Distelfeld A, McGuire PE, Dvorak J, Luo M-C. Improved genome sequence of wild emmer wheat Zavitan with the aid of optical maps. G3: Genes Genomes Genet. 2019;9(3):619–24.
20. Kim D, Paggi JM, Park C, Bennett C, Salzberg SL. Graph-based genome alignment and genotyping with HISAT2 and HISAT-genotype. Nat Biotechnol. 2019;37(8):907–15.
21. Li H. A statistical framework for SNP calling, mutation discovery, association mapping and population genetical parameter estimation from sequencing data. Bioinformatics. 2011;27(21):2987–93.
22. Van der Auwera GA, O'Connor BD. Genomics in the Cloud: Using Docker, GATK, and WDL in Terra. O'Reilly Media; 2020.
23. Danecek P, Auton A, Abecasis G, Albers CA, Banks E, DePristo MA, Handsaker RE, Lunter G, Marth GT, Sherry ST, et al. The variant call format and VCFtools. Bioinformatics. 2011;27(15):2156–8.
24. Adhikari L, Raupp J, Wu S, Wilson D, Evers B, Koo DH, Singh N, Friebe B, Poland J. Genetic characterization and curation of diploid A-genome wheat species. Plant Physiol. 2022;188(4):2101–14.
25. Endelman JB. Ridge Regression and Other Kernels for Genomic Selection with R Package rrBLUP. Plant Genome. 2011;4(3):250–5.
26. Team RC. R: A language and environment for statistical computing. In.; 2023.
27. Frichot E, François O. LEA: An R package for landscape and ecological association studies. Methods Ecol Evol. 2015;6(8):925–9.
28. Francis RM. POPHELPER: an R package and web app to analyse and visualize population structure. Mol Ecol Resour. 2017;17(1):27–32.
29. Nei M. Analysis of gene diversity in subdivided populations. Proc Natl Acad Sci. 1973;70(12):3321–3.
30. Weir BS, Cockerham CC. Estimating F-statistics for the analysis of population structure. Evolution. 1984:1358–70.
31. Weir BS, Goudet J. A Unified Characterization of Population Structure and Relatedness. Genetics. 2017;206(4):2085–103.
32. Nei M. Molecular evolutionary genetics. Columbia university; 1987.
33. Kassambara A. Ggplot2: guide to create beautiful graphics in R. Alboukadel KASSAMBARA; 2013.
34. Lipka AE, Tian F, Wang Q, Peiffer J, Li M, Bradbury PJ, Gore MA, Buckler ES, Zhang Z. GAPIT: genome association and prediction integrated tool. Bioinformatics. 2012;28(18):2397–9.
35. Wang J, Zhang Z. GAPIT Version 3: Boosting Power and Accuracy for Genomic Association and Prediction. Genom Proteom Bioinform. 2021;19(4):629–40.
36. Sayers EW, Bolton EE, Brister JR, Canese K, Chan J, Comeau DC, Connor R, Funk K, Kelly C, Kim S, et al. Database resources of the national center for biotechnology information. Nucleic Acids Res. 2022;50(D1):D20–6.
37. Poyarkova H. Morphology, geography and infraspecific taxonomics of Triticum dicoccoides Körn. A retrospective of 80 years of research. Euphytica. 1988;38(1):11–23.
38. Poyarkova H, Gerechter-Amitai ZK, Genizi A. Two variants of wild emmer (*Triticum dicoccoides*) native to Israel: morphology and distribution. Can J Bot. 1991;69(12):2772–89.
39. Jorgensen C, Luo M-C, Ramasamy R, Dawson M, Gill BS, Korol AB, Distelfeld A, Dvorak J. A High-density genetic map of wild emmer wheat from the Karaca Dağ Region provides new evidence on the structure and evolution of wheat chromosomes. Front Plant Sci. 2017;8:1798.
40. Luo MC, Yang ZL, You FM, Kawahara T, Waines JG, Dvorak J. The structure of wild and domesticated emmer wheat populations, gene flow between them, and the site of emmer domestication. Theor Appl Genet. 2007;114(6):947–59.
41. Mastrangelo AM, Roncallo P, Matny O, Čegan R, Steffenson B, Echenique V, Šafář J, Battaglia R, Barabaschi D, Cattivelli L et al. A new wild emmer wheat panel allows to map new loci associated with resistance to stem rust at seedling stage. Plant Genome. 2023;n/a(n/a):e20413
42. Özkan H, Brandolini A, Schäfer-Pregl R, Salamini F. AFLP analysis of a collection of tetraploid wheats indicates the origin of emmer and hard wheat domestication in southeast Turkey. Mol Biol Evol. 2002;19(10):1797–801.
43. Lev-Yadun S, Gopher A, Abbo S. The cradle of agriculture. Science. 2000;288(5471):1602–3.
44. Blumler MA. Introgression of durum into wild emmer and the agricultural origin question. In: The origins of agriculture and crop domestication Proc Harlan Symp: 1998; Aleppo, Syria. Published jointly by ICARDA, IPGRI, FAO, and UC/GRCP; 1998: 252–268.
45. Huang L, Raats D, Sela H, Klymiuk V, Lidzbarsky G, Feng L, Krugman T, Fahima T. Evolution and Adaptation of Wild Emmer Wheat Populations to Biotic and Abiotic Stresses. Annu Rev Phytopathol. 2016;54(1):279–301.
46. Lhamo D, Sun Q, Zhang Q, Li X, Fiedler JD, Xia G, Faris JD, Gu Y-Q, Gill U, Cai X, et al. Genome-wide association analyses of leaf rust resistance in cultivated emmer wheat. Theor Appl Genet. 2023;136(1):20.
47. Letta T, Olivera, Maccaferri M, Jin Y, Ammar K, Badebo A, Salvi S, Noli E, Crossa J, Tuberosa R. Association Mapping Reveals Novel Stem Rust Resistance Loci in Durum Wheat at the Seedling Stage. Plant Genome. 2014;7(1):plantgenome201320080026.
48. Megerssa SH, Ammar K, Acevedo M, Brown-Guedira G, Ward B, Degete AG, Randhawa MS, Sorrells ME. Multiple-Race Stem Rust Resistance Loci Identified in Durum Wheat Using Genome-Wide Association Mapping. Front Plant Sci. 2020;11:598509.
49. Singh A, Pandey MP, Singh AK, Knox RE, Ammar K, Clarke JM, Clarke FR, Singh RP, Pozniak CJ, Depauw RM, et al. Identification and mapping of leaf, stem and stripe rust resistance quantitative trait loci and their interactions in durum wheat. Mol Breed. 2013;31(2):405–18.
50. Herrera-Foessel S, Huerta-Espino J, Calvo-Salazar V, Lan C, Singh R. Lr72 confers resistance to leaf rust in durum wheat cultivar Atil C2000. Plant Dis. 2014;98(5):631–5.
51. Wang F, Zhang M, Hu Y, Gan M, Jiang B, Hao M, Ning S, Yuan Z, Chen X, Chen X, et al. Pyramiding of Adult-Plant Resistance Genes Enhances All-Stage Resistance to Wheat Stripe Rust. Plant Dis. 2023;107(3):879–85.
52. Wang J, Tao F, Tian W, Guo Z, Chen X, Xu X, Shang H, Hu X. The wheat WRKY transcription factors TaWRKY49 and TaWRKY62 confer differential high-temperature seedling-plant resistance to Puccinia striiformis f. sp. tritici. PLoS ONE. 2017;12(7):e0181963.
53. Hawku MD, Goher F, Islam MA, Guo J, He F, Bai X, Yuan P, Kang Z, Guo J. TaAP2-15, An AP2/ERF transcription factor, is positively involved in wheat resistance to Puccinia striiformis f. sp. tritici. Int J Mol Sci. 2021;22(4):2080.
54. Peng JH, Fahima T, Röder, Huang QY, Dahan A, Li YC, Grama A, Nevo E. High-density molecular map of chromosome region harboring stripe-rust resistance genes YrH52 and Yr15 derived from wild emmer wheat, *Triticum dicoccoides*. Genetica. 2000;109(3):199–210.
55. Klymiuk V, Fatiukha A, Fahima T. Wheat tandem kinases provide insights on disease-resistance gene flow and host-parasite co-evolution. Plant J. 2019;98(4):667–79.
56. Alam MA, Mandal M, Wang C, Ji W. Chromosomal location and SSR markers of a powdery mildew resistance gene in common wheat line N0308. Afr J Microbiol Res. 2013;7(6):477–82.
57. Xie CJ, Ni ZF, Sun QX, Yang ZM, Liu BS, Wei YL. [Molecular tagging of a major powdery mildew resistance gene MlG in wheat derived from wild Emmer by using microsatellite marker]. Yi Chuan Xue Bao. 2001;28(11):1034–9.
58. Wei ZZ, Klymiuk V, Bocharova V, Pozniak C, Fahima T. A Post-Haustorial Defense Mechanism is Mediated by the Powdery Mildew Resistance Gene, PmG3M, Derived from Wild Emmer Wheat. Pathogens. 2020;9(6):418.
59. Xie W, Nevo E. Wild emmer: genetic resources, gene mapping and potential for wheat improvement. Euphytica. 2008;164(3):603–14.
60. Bischoff V, Nita S, Neumetzler L, Schindelasch D, Urbain A, Eshed R, Persson S, Delmer D, Scheible WR. TRICHOME BIREFRINGENCE and its homolog AT5G01360 encode plant-specific DUF231 proteins required for cellulose biosynthesis in Arabidopsis. Plant Physiol. 2010;153(2):590–602.
61. Sharma Poudel R, Al-Hashel AF, Gross T, Gross P, Brueggeman R. Pyramiding rpg4- and Rpg1-Mediated Stem Rust Resistance in Barley Requires the Rrr1 Gene for Both to Function. Front Plant Sci. 2018;9:1789.

Publisher's note